Raman Spectroscopy of Mercury(II) Binding to Two Filamentous Viruses: Ff (fd, M13, f1) and Pf1†

Loren A. Day,*,‡ Arturo Casadevall,‡ Betty Prescott,§ and George J. Thomas, Jr.*,§

The Public Health Research Institute of the City of New York, 455 First Avenue, New York, New York 10016, and Division of Cell Biology and Biophysics, University of Missouri—Kansas City, Kansas City, Missouri 64110

Received June 24, 1987; Revised Manuscript Received August 31, 1987

ABSTRACT: Ff and Pf1 are filamentous bacteriophages. Each contains, in a central core region surrounded by protein, a circular single-stranded DNA molecule, and it is known that the DNA bases are sites of Hg(II) binding. In the present study, Raman spectra were obtained for the two viruses in the presence of increasing amounts of Hg(II), with ratios (m) of Hg(II) added per nucleotide residue in the range $0 < m < 2.0$. Hg(II) binding to the viruses induces Raman intensity changes in previously assigned Raman lines of viral DNA, demonstrating metal binding to the DNA bases, but also in many lines assigned to protein. The overall structures of the viruses do not change with Hg(II) binding, and the Raman spectra indicate little, if any, change in protein secondary structure. Changes in certain protein Raman lines induced by Hg(II) binding to the DNA for low values of m are attributed to altered interactions between solvent and protein side chains, aliphatic groups being the most affected. The nature of such changes for both viruses suggests DNA–protein linkage. In Pf1, lines assigned to ring vibrations of all four bases are perturbed upon initial addition of Hg(II) to $m = 0.25$. In Ff, however, lines assigned to base ring vibrations are not perturbed until $m \geq 0.5$. The results provide additional evidence for fundamentally different DNA structures in Ff and Pf1.

The filamentous bacteriophages are the longest and thinnest known viruses. They consist of a circular, single-stranded DNA molecule packed in a cylindrical coat of thousands of identical protein subunits with a few copies of minor coat proteins at the ends. Ff and Pf1 are the two viruses for which the most structural data are available (Makowski, 1984; Marvin et al., 1987; Day et al., 1988), but a complete structure has not yet been established for either one. In particular, neither of the DNA structures in the virions has been solved, although many techniques have been applied to the problem (Day, 1969; Frank & Day, 1970; Thomas & Murphy, 1975; Day et al., 1979, 1988; Banner et al., 1981; DiVerdi & Opella 1981; Ikoku & Hearst, 1981; Webster et al., 1981; Casadevall & Day, 1982, 1983; Cross et al., 1983; Thomas et al., 1983; Marzec & Day, 1983). One approach has been to use Ag(I) and Hg(II) salts as probes of DNA structure (Casadevall & Day, 1982, 1983). These metal ions penetrate through the protein coats of the viruses and bind to the DNA where they cause large changes in circular dichroism (CD)[1] spectra. Little if any direct binding of the metal ions to the coat protein is believed to occur since the subunits lack groups, such as sulfhydryls, that can compete with DNA bases. Accordingly, minimal changes in protein CD bands occur upon Ag(I) or Hg(II) binding. The UV absorbance, CD, and NMR results have been interpreted to indicate that the orientations of DNA in Ff and Pf1 are fundamentally different from one another, and models based on available data have been proposed (Day et al., 1979, 1988; Casadevall & Day, 1982, 1983; Cross et al., 1983; Marzec & Day, 1983). Additional information on the accessibility of Ff and Pf1 DNA bases to site-specific reagents is expected from Raman spectra, which contain large numbers of structure-sensitive vibrational lines due to protein and DNA constituents (Thomas, 1987).

Previous applications of Raman spectroscopy to the filamentous viruses have yielded information on the secondary structures of their protein and DNA components, and on structure perturbations and transitions as functions of temperature and ionic strength (Thomas & Murphy, 1975; Thomas & Day, 1981; Thomas et al., 1983). In this paper, we present our initial findings on changes induced by Hg(II) to the Raman spectra of Ff and Pf1. Our aim was to study the Hg–virus derivatives with Raman spectroscopy to define better the usefulness of Hg(II) as a structure probe in these systems. Some of the Raman spectral changes are interpreted in terms of altered protein–solvent interactions. Others are assigned to perturbation of DNA Raman lines which, although complicated in some cases by overlap from protein Raman lines, show distinct differences in the modes of Hg(II) binding to the DNA genomes in the two viruses.

Materials and Methods

The particular Ff virus used in this study was fd, the major coat protein sequence of which is identical with that of f1 but differs from that of M13 in position 12. [See, for example, Putterman et al. (1984) for the sequences.] Solutions of fd and Pf1 viruses and their Hg(II) derivatives, prepared by complexation with mercury(II) acetate as described previously, yielded UV absorbance and CD spectra like those reported (Casadevall & Day, 1983). For Raman spectroscopy the solutions were pelleted by ultracentrifugation and resuspended to final concentrations in the range 60–100 mg/mL (10–40 mM in nucleotides). The ratios of moles of Hg(II) added per mole of nucleotides were in the range $0 < m < 2.0$. The buffer was 150 mM borate, pH 8.6 (83 mM in Na^+ and 150 mM

† Part XXII in the series "Studies of Virus Structure by Raman Spectroscopy" (G.J.T.) and part of a series on the physical properties of filamentous viruses (L.A.D.). This research was supported by NIH Grants AI 09049 (L.A.D.) and AI 11855 (G.J.T.).

‡ The Public Health Research Institute of the City of New York.
§ University of Missouri—Kansas City.

[1] Abbreviations: CD, circular dichroism; m, ratio of moles of Hg(II) added per mole of nucleotide present; UV, ultraviolet.

0006-2960/88/0427-0706$01.50/0

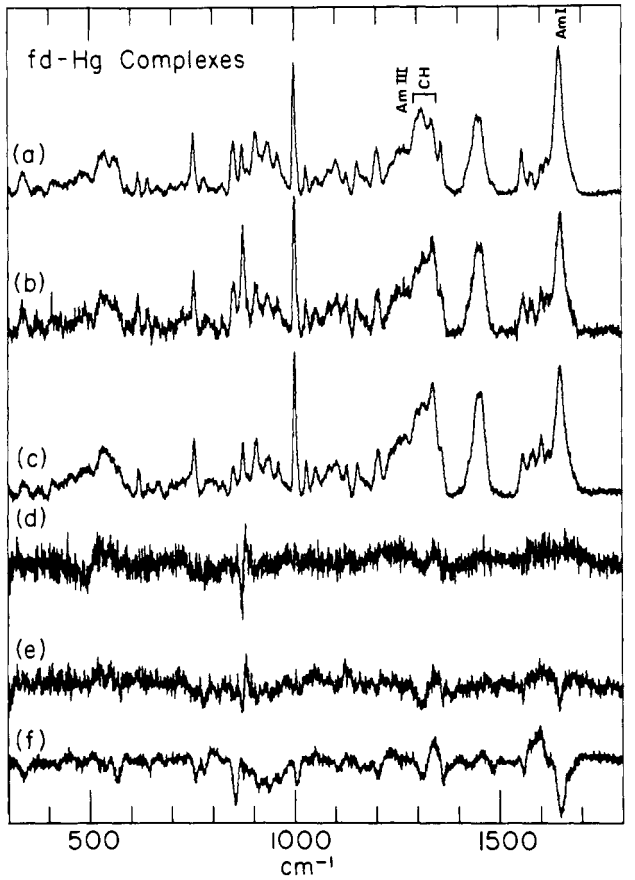

FIGURE 1: Raman spectra in the region 300–1800 cm^{-1} of fd virus in 150 mM borate buffer at 20 °C for different ratios (m) of Hg(II) added per DNA nucleotide of the virus. (a) $m = 0.0$; (b) $m = 0.50$; (c) $m = 2.0$; (d) difference spectrum ($m = 0.25$) – ($m = 0.0$); (e) difference spectrum ($m = 0.50$) – ($m = 0.0$); (f) difference spectrum ($m = 2.0$) – ($m = 0.0$).

in borate species), prepared by mixing 0.15 M boric acid and 0.15 M $Na_2B_4O_7$ in a volume ratio of 45:55. The same buffer was used in earlier CD studies. The virus and Hg–virus samples were sealed in glass capillaries (Kimax 34507) and thermostated at 20 ± 0.5 °C (Thomas & Barylski, 1970). Other details of sample handling have been described (Thomas et al., 1983).

The 514.5-nm argon line from a Spectra-Physics Model 171-18 laser was used for excitation of Raman spectra, employing approximately 200 mW of radiant power at the sample. Spectra were collected on a Spex Ramalog V/VI spectrometer under the control of a North Star Horizon HRZ-2-64K-Q microcomputer, with a spectral slit width of 8 cm^{-1} and integration time of 1 s for photon counts at increments of 1.0 cm^{-1}. No smoothing or filtering of data was employed. The Raman spectra used in the analysis were the averages of repeated scans (8 of the 300–1800-cm^{-1} region and 30 of the 600–845-cm^{-1} region). The spectra were corrected for scattering by the solvent and buffer and for the gently sloping background characteristics of aqueous solution spectra of viruses. Because of the low weight percent composition of DNA in each of the viruses, 6% in Pf1 and 12% in fd, the Raman lines of the DNA are among the weakest in the spectra and signal-to-noise ratios are relatively low despite the signal averaging employed. This is particularly evident in difference spectra of the 600–845-cm^{-1} region (shown below), which reflects primarily the Raman scattering from vibrations of subgroups of the encapsidated DNA molecules.

The perturbations produced by Hg(II) binding have been analyzed with the aid of difference spectra. Each has been

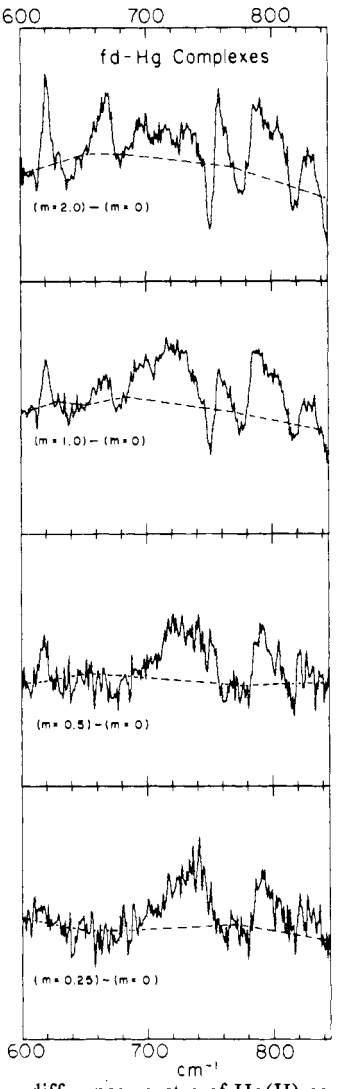

FIGURE 2: Raman difference spectra of Hg(II) complexes of fd in the region 600–845 cm^{-1} for various values of m as indicated.

obtained by computer subtraction of the spectrum of the native virus (at $m = 0.0$), as subtrahend, from the spectrum of the Hg(II) derivative ($0.25 < m < 2.0$), as minuend. Accordingly, positive bands in the difference spectra correspond to Raman lines which have gained intensity as a consequence of Hg(II) binding, and conversely for negative bands. The base lines for the difference spectra in the 600–845-cm^{-1} spectral region (Figures 2 and 4) were obtained by first finding all the frequencies (cm^{-1} values or abscissas) at which zero amplitudes (or very deep minima) occur simultaneously both in the spectrum of a virus in the absence of Hg(II) and in a spectrum of that virus in the presence of a particular concentration of Hg(II). The amplitude at each of these frequencies in the difference spectrum for this pair of spectra was assigned the value zero. The complete base lines, not straight for any of the spectra of Figures 2 and 4, were then constructed by connecting successive zero-amplitude points with straight line segments.

RESULTS

Addition of Hg(II) to solutions of the viruses in 150 mM borate buffer resulted in significant Raman intensity changes, affecting both DNA and protein Raman lines. This is shown for fd in Figures 1 and 2 and for Pf1 in Figures 3 and 4. In spite of the many spectral changes, we note specifically that the overall structures of the viruses, as observed by electron microscopy, analytical ultracentrifugation, and CD spectros-

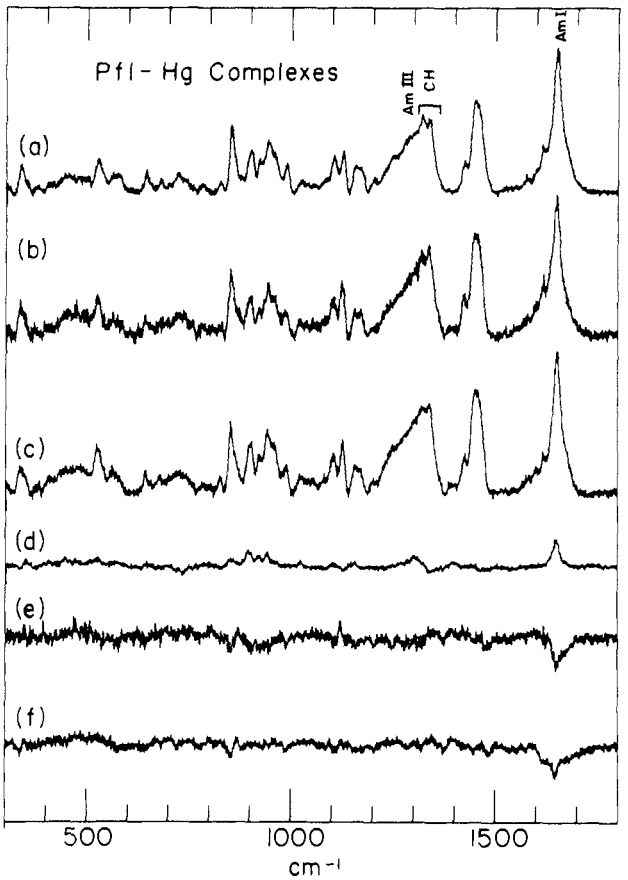

FIGURE 3: Raman spectra in the region 300–1800 cm^{-1} of Pf1 for different ratios (m) of Hg(II) added per DNA nucleotide of the virus. (a) m = 0.0; (b) m = 1.0; (c) m = 2.0; (d) difference spectrum (m = 0.25) − (m = 0.0); (e) difference spectrum (m = 1.0) − (m = 0.0); (f) difference spectrum (m = 2.0) − (m = 0.0). Other conditions as Figure 1.

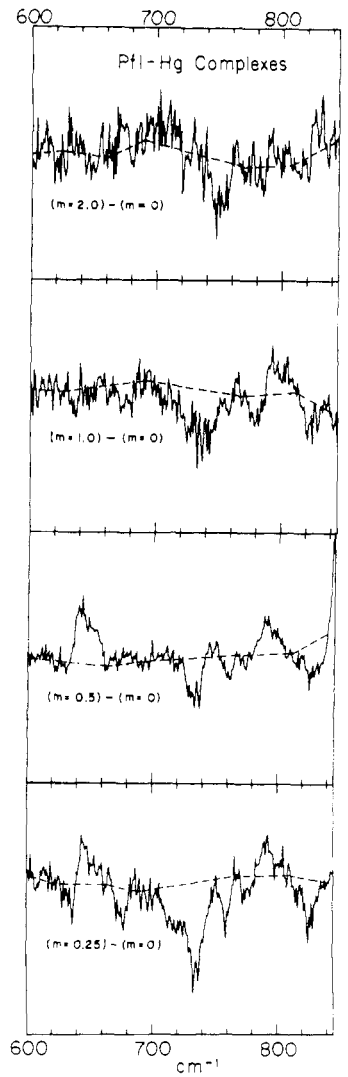

FIGURE 4: Raman difference spectra of Hg(II) complexes of Pf1 in the region 600–845 cm^{-1} for various values of m as indicated.

copy, do not change (Casadevall & Day, 1982, 1983; Reisberg, 1988). They remain highly α-helical in protein conformation, and the frequencies of the Raman DNA bands do not change. The altered Raman amplitudes are considered to reflect perturbations of the native structures.

Our analysis of the data of Figures 1–4 depends on earlier results for the filamentous viruses and for Hg–cytidine and Hg–adenine complexes. Raman lines for DNA and protein in both viruses have been assigned, and it was observed that changes in NaCl concentration cause changes in certain Raman lines of the protein (Thomas et al., 1983). In particular, changes in salt concentration induce changes in several bands assigned to CH, CH_2, and CH_3 deformation modes. Bands in the 710–750-cm^{-1} region that change with salt concentration were assigned in part to changes in adenine ring vibrations. We now assign the NaCl-induced changes at about 735 cm^{-1} primarily to CH_2 and CH_3 vibrational modes (Bellamy, 1975). In the present study, all spectra were obtained in 150 mM borate buffer. In this buffer the Raman spectra of the two native viruses in the absence of Hg(II) (Figures 1 and 3) are similar to the so-called "high-salt" spectra obtained earlier in 150 mM NaCl and 10 mM $Na_2B_4O_7$ (Thomas et al., 1983; comparisons not shown). For the two viruses, it was established by CD and UV absorbance that Hg(II) binds directly to the bases and that changes in binding modes occur for fd at about m = 0.5 and for Pf1 at about m = 1.0 (Casadevall & Day, 1982, 1983). Although some Hg(II) binding to protein cannot be excluded, the lack of sulfhydryl groups in the coat protein argues against significant competition between protein and the bases at low values of m. There is no evidence, spectral or otherwise, for Hg(II) binding to sites other than sites on bases in these viruses.

Hg(II) is known to bind with high affinity to DNA, polynucleotides, and nucleotides at the level of the bases, and no binding is believed to occur at the level of the phosphates (Yamane & Davidson, 1961; Simpson, 1963; Young et al., 1982; Keller & Hartman, 1985). Hg(II) binding to cytidine decreases intensity at 778 cm^{-1} and increases intensity at 1250 cm^{-1} (Lord & Thomas, 1967). Raman effects of Hg(II) binding to poly(rA) (this study, spectra not shown) are like those of Hg(II) binding to adenine and to ATP, with intensity increases near 1324 and 1406 cm^{-1} and intensity decreases near 725, 1301, and 1336 cm^{-1}; in addition, frequency shifts occur from 1480 to 1489 cm^{-1} and from 1574 to 1562 cm^{-1} (Lanir & Yu, 1979; Marzilli et al., 1980). Some of these spectral fingerprints of Hg–Cyt and Hg–Ade coordination are detectable within the complex profiles of Raman lines in fd and Pf1 virus spectra.

Analysis for fd Virus. The initial addition of Hg(II) to m = 0.25 [the equivalent of 1 Hg(II) for 83 amino acids] perturbed only Raman lines that have been assigned to several side chain vibrations of the protein, even though the Hg(II) is binding to the DNA bases. This is evident in the difference spectrum of Figure 1d where a negative band near 1301 cm^{-1} (CH_2 twist/wag) and a positive band near 1340 cm^{-1} (also CH_2 twist/wag) are discernible. In Figure 1d, the slight

intensity increase in amide I (1645–1655 cm^{-1}) is attributable to imperfect solvent compensation, and the absence of intensity change in the amide III region (ca. 1275 cm^{-1}), confirms no change in protein secondary structure. However, changes in the low-frequency region 510–580 cm^{-1} from skeletal modes of α-helix are observed (Figure 1d). A change in the line at 875 cm^{-1} assigned to Trp is also observed, possibly with a frequency shift. Slight changes in Phe (1000, 1030, and 1203 cm^{-1}) are discernible. Figure 2 shows that the initial increment affects the broad band from CH_2 and CH_3 deformation modes near 735 cm^{-1}. We find it significant that very similar changes were observed in the difference spectrum for the transfer of fd from "high-salt" buffer (150 mM NaCl, 10 mM $Na_2B_4O_7$) to "low-salt" buffer (1 mM $Na_2B_4O_7$). These changes were attributed to altered protein–solvent interactions at the different salt concentrations (Thomas et al., 1983). The signs of the amplitude changes for the two difference spectra [Figure 1d here and Figure 2b of Thomas et al. (1983)] are *opposite*; that is, the *increase* in Hg acetate concentration produces amplitude changes in the directions produced by a *decrease* in NaCl concentration.

The initial increment of Hg(II) to $m = 0.25$ does not produce discernible changes in any lines assigned to DNA ring vibrations, but there are changes in DNA backbone vibrations. DNA lines, free of protein contributions, have been assigned for fd at 667 (Thy), 674 (Gua), 724 (Ade), 747 (Thy), 779 (Cyt), 802 (phosphodiester backbone), 1486 (Ade, Gua), and 1529 cm^{-1} (Ade, Cyt) by Thomas et al. (1983; see Figure 1a and Table 3 of that paper and Figure 1a here). Our analysis of the changes is focused in the 600–845-cm^{-1} spectral region where many ring vibrations occur (Figure 2). There is no discernible change in the range 660–680 cm^{-1} (Thy, Gua), and there is no change at 779 cm^{-1} (Cyt). Ring vibrations at 742 (Ade) and 747 cm^{-1} (Thy) are overlapped by the broad difference band for CH_2 and CH_3 deformation modes assigned above. Also, no changes are discernible at 1486 (Ade, Gua) and 1524 cm^{-1} (Ade, Cyt). The asymmetric difference band with a maximum at 790 cm^{-1} and a shoulder at 804 cm^{-1} is due primarily to altered intensity of a phosphodiester OPO stretching mode of the DNA backbone. Thus, the initial increment of Hg(II) produces no discernible or assignable perturbations of ring vibrations of the bases in the 600–845-cm^{-1} region but does perturb bands associated with vibrations of the backbone and protein side chains, even though it is known from absorbance and CD that the Hg(II) is bound to the bases.

For $m \geq 1.0$, the changes in DNA backbone intensities persist at 790 cm^{-1} and become stronger at 804 cm^{-1}. There is now a clear change in Gua and/or Thy intensity in a broad band centered at 668 cm^{-1}. An intensity decrease at about 776 cm^{-1} (Cyt) appears for $m \geq 1.0$, but concomitant changes in 1250 cm^{-1} (Cyt) are not apparent, perhaps obscured by protein. The Ade band at 724 cm^{-1} is obscured by the breadth of the 735-cm^{-1} protein band. The diminished positive intensity centered at about 720 cm^{-1} at $m = 2.0$ would seem to indicate that a decreasing 724-cm^{-1} Ade line compensates the increased intensity from the overlapping 735-cm^{-1} protein band. In summary, for fd DNA, Raman lines of the backbone though not of the bases undergo perturbations at $m = 0.25$; at $m = 0.5$ possible slight changes in Gua and Ade are discernible, but not in Cyt, and backbone perturbations are not changed further; at $m = 1.0$ and 2.0, perturbations in all distinct bands of the DNA bases are evident.

For $m = 2.0$, changes in fd protein lines assigned to aromatic groups are clearly seen (Figure 1f), at 620 (Phe), 641 (Tyr), 754 (Trp), 853 (Tyr), 1000 (Phe), 1200 (Tyr, Phe), 1558 (Trp), and 1591 cm^{-1} (Phe, Tyr), probably indicating major changes to protein packing in the virus. Protein conformation may also have changed at this high value of m, as indicated by significant asymmetry in the amide I negative difference band (centered at 1647 cm^{-1}) and corresponding positive difference band in the amide III region (1230–1270 cm^{-1}). These amide band perturbations are consistent with conversion of helical secondary structure to nonhelical secondary structure.

Analysis for Pf1 Virus. The initial addition of Hg(II) to $m = 0.25$ [equivalent to one Hg(II) for every 200 amino acids] causes changes in Raman lines of both protein side chain groups and DNA base residues. The changes in protein lines show remarkable similarity to those induced by NaCl. The difference spectrum (Figure 3d) shows a positive band at about 1302 cm^{-1}, a negative band near 1340 cm^{-1}, and a negative band at 735 cm^{-1}, all of which we assign to aliphatic side chains. The positive difference intensities in helix amide I (1650 cm^{-1}) and possibly also amide III (ca. 1275 cm^{-1}) suggest anisotropy in the Raman scattering, since the former is highly symmetrical in shape, and no corresponding negative difference intensities are evident at the amide I (1660–1670 cm^{-1}) and amide III (1230–1260 cm^{-1}) frequencies diagnostic of nonhelix structure. Therefore, no change of subunit secondary structure occurs. The spectrum of Figure 3d mimics the difference spectrum obtained for Pf1 in high salt relative to low salt [see Figure 2a of Thomas et al. (1983)]. In contrast to the case for fd, the signs of the amplitude changes for the two difference spectra [Figure 3d here and Figure 2a of Thomas et al. (1983)] are *the same*. However, addition of Hg(II) to Pf1 beyond $m = 0.5$ reverses the direction of perturbations. The reversal is evident from comparisons of difference spectra d–f of Figure 3. Other significant changes in the protein Raman lines of Pf1, resulting from excess Hg(II), are intensity increases near 870 cm^{-1} (Val) and decreases near 853 (Tyr), 987 (Ile), and 1616 cm^{-1} (Tyr). Asymmetry in the negative amide I difference band and the accompanying changes in the amide III region both suggest some loss of α-helical secondary structure at the highest value of m (Figure 3f).

The first addition of Hg(II) ($m = 0.25$) to Pf1 appears to cause changes in ring vibrations of all four bases and in the phosphodiester backbone, but there are curious reversal effects on subsequent additions. Lines that have been assigned to DNA in Pf1 spectra are 661 (Thy), 679 (Gua), 723 (Ade), 746 (Thy), 782 (Cyt), 1489 (Ade, Gua), and 1528 cm^{-1} (Ade, Cyt), according to Thomas et al. (1983); in addition, a more recent analysis assigns an asymmetric tail to the 746-cm^{-1} line for Thy extending to about 767 cm^{-1} (Thomas et al., 1988). Difference spectra in the 600–845-cm^{-1} spectral region are shown in Figure 4. A slight increase is discerned at 661 cm^{-1} (Thy) and a clear decrease is seen at 679 cm^{-1} (Gua). A shoulder at 720 cm^{-1} on the 735-cm^{-1} aliphatic side chain band is assigned to Ade. The clear decrease at 760 cm^{-1} is tentatively assigned to Thy, and the small decrease over 770–782 cm^{-1} is ascribed to Cyt. The increase at 790 cm^{-1} is assigned to a change in backbone vibrations. These backbone effects remain about the same for increases in Hg(II) to $m = 1.0$ but are reversed to zero difference by $m = 2.0$. Reversals in changes assigned to base ring vibrations occur already at $m = 0.5$; only a very small negative difference is seen at 760 cm^{-1} (Thy) which then disappears by $m = 1.0$. Small bands at 680 and 780 cm^{-1} (Gua and Cyt) which have disappeared at $m = 0.5$ seem to reappear at $m = 1.0$, only to disappear into noise at $m = 2.0$. These effects, seen with the aid of extensive signal

averaging for the 600–845-cm^{-1} region, are accompanied by the changes in protein lines with reversals, described above, over the entire spectral region investigated (Figure 3). In addition, bands assigned to tyrosine (640–660 and 829 cm^{-1}) undergo changes at low m values that are reversed at high m values (Figure 4).

Discussion

The Hg derivatives of Pf1 and fd showed no photodegradation under the conditions used in this study. We also attempted to study Ag(I) derivatives of fd and Pf1, for comparison with the present results and with previously described CD results (Casadevall & Day, 1983), but photodegradation of Ag(I) derivatives by laser illumination could not be avoided. The Hg(II)-induced Raman intensity changes were small, and signal averaging was necessary to enhance the signal-to-noise ratios. Although some difference spectra at low values of m have low signal-to-noise ratios, subtle changes induced by Hg(II) could be discerned and assigned to Hg(II) binding. The changes induced by Hg(II) in the Raman spectra of these viruses are complex.

The results provide additional evidence for fundamentally different DNA structures in Ff and Pf1. Initial increments of Hg(II) appear to produce changes in lines assigned to ring vibrations of all the bases in Pf1 but none in Ff. In the case of Pf1, there appear to be sign reversals in the Raman intensity changes on subsequent additions of Hg(II). Changes in UV absorbance are monotonic for both viruses, but CD changes undergo a sign reversal for Ff, not Pf1 (Casadevall & Day, 1983). Detailed mechanisms for the two different Raman results must await the accrual of additional reference data, but at present we offer the following explanation. It has been proposed that Hg(II) binding to Ff leads to the formation of Hg bridges between bases in the two antiparallel DNA strands (Casadevall & Day, 1983), and such bridging would be accompanied by the displacement of protons from hydrogen bonding positions between these bases, whether the hydrogen bonding is of the Watson–Crick type or not. Raman spectra show that similar perturbations of cytosine and adenine ring vibrations result from Hg(II) and proton binding (Lord & Thomas, 1967; Lanir & Yu, 1979). Thus, the initial increment of Hg(II) to Ff could displace protons at ring sites without producing changes in Raman lines assigned to ring vibrations. Hg(II) binding to Pf1, on the other hand, is characterized by entirely different CD changes and is thought not to lead to bridge formation (Casadevall & Day, 1983). The bases are expected to be free for Hg(II) at all sites, so that Raman changes could be similar to Raman changes for nucleotides and single-stranded polynucleotides, as appears to be the case.

Hg(II) binding causes intensity changes to many Raman lines for protein, but no major change of protein secondary structure is observed. This is consistent with the previous observation that Hg(II) causes only small changes in the protein CD bands of these viruses (Casadevall & Day, 1982, 1983). We cannot rule out some Hg(II) binding to the protein at the higher values of m when sites on the bases are occupied. However, at $m = 0.25$ Hg(II) is bound to the bases. Given this, an unexpected finding was the similarity between Raman spectral changes caused by Hg(II) binding and those caused by changes in NaCl concentration. Except for the very small intensity differences in DNA lines, and possibly in tyrosine lines (829, 854 cm^{-1}), the difference spectrum generated by subtracting the spectrum of Pf1 from that of Hg–Pf1 at $m = 0.25$ is virtually superimposable on the difference spectrum generated by subtracting the spectrum of Pf1 in 1 mM $Na_2B_4O_7$ from its spectrum in 150 mM NaCl and 10 mM $Na_2B_4O_7$ [see Thomas et al. (1983), Figure 2a]. The corresponding difference spectra for Ff (which unfortunately suffer from higher noise levels) also show a close similarity, if not superimposablity, except that the sign is reversed [Figure 1d here and Figure 2b in Thomas et al. (1983)]. The closeness of these difference spectra implies close similarity in the types of structural perturbations for the two conditions, even though Hg(II) binds to the bases and NaCl does not. The NaCl-induced Raman intensity changes were interpreted earlier (Thomas et al., 1983) as resulting from changes in solvent accessibility of the coat protein.

Separate from the issues of DNA structure differences and protein side chain perturbations are questions of DNA–protein interactions and linkage. We propose, as a working hypothesis for Ff, that the changes in the protein lines result from a structure perturbation attendant with Hg(II) binding to the bases that is transmitted through the DNA backbone to the protein. This would explain the simultaneity of changes in aliphatic and amide group protein lines and DNA backbone lines, without apparent changes in ring vibrations. For Pf1, on the other hand, changes in base ring vibrations and protein side chain vibrations are all simultaneous at $m = 0.25$. At $m \geq 0.5$, the direction of the intensity changes in many of the Pf1 protein lines changes, as is the case for the DNA lines. The reversals, like the initial effects, are not understood but must be induced primarily by continued binding of Hg(II) to the bases. Also, at higher Hg(II) ratios other protein lines change, indicating additional perturbations of the protein structure.

In summary, Hg(II) binds to these viruses with little change in overall virus structure or protein secondary structure and hence is a good DNA structure probe for use in spectroscopy and X-ray fiber diffraction. Raman spectroscopy appears to be very sensitive to small changes in DNA–protein structure in these systems. The Raman results indicate different Hg–base complexes in these viruses and provide further evidence for the existence of very different types of DNA structures. Although unequivocal assignments to base residues are difficult because of overlapping protein lines, there is little doubt that Hg(II) is binding differently to the DNAs inside fd and Pf1.

References

Banner, D., Nave, C., & Marvin, D. A. (1981) *Nature (London) 289*, 814–816.

Bellamy, L. J. (1975) *The Infrared Spectra of Complex Molecules*, Vol. 1, 3rd ed., Wiley, New York.

Casadevall, A., & Day, L. A. (1982) *Nucleic Acids Res. 10*, 2467–2481.

Casadevall, A., & Day, L. A. (1983) *Biochemistry 22*, 4831–4842.

Cross, T. A., Tsang, P., & Opella, S. J. (1983) *Biochemistry 22*, 721–726.

Day, L. A. (1969) *J. Mol. Biol. 39*, 265–277.

Day, L. A., & Wiseman, R. L. (1978) in *The Single-Stranded DNA Phages* (Denhardt, D. T., Dressler, D., & Ray, D. S., Eds.) pp 605–675, Cold Spring Harbor Laboratory Press, Cold Spring Harbor, NY.

Day, L. A., Wiseman, R. L., & Marzec, C. J. (1979) *Nucleic Acids Res. 7*, 1393–1403.

Day, L. A., Marzec, C. J., Reisberg, S. A., & Casadevall, A. (1988) *Annu. Rev. Biophys. Biophys. Chem.* (in press).

DiVerdi, J. A., & Opella, S. J. (1981) *Biochemistry 20*, 280–284.

Frank, H., & Day, L. A. (1970) *Virology 42*, 144–154.

Fritzche, H., Cross, T. A., Opella, S. J., & Kallenbach, N. R. (1981) *Biophys. Chem. 14*, 283–291.

Ikoku, A. S., & Hearst, J. E. (1981) *J. Mol. Biol. 151*, 245–255.
Keller, P. B., & Hartman, K. A. (1985) *Spectrochim. Acta, Part A 42A*, 299–306.
Lanir, A., & Yu, N.-T. (1979) *J. Biol. Chem. 254*, 5882–5887.
Lord, R. C., & Thomas, G. J. (1967) *Spectrochim. Acta, Part A 23A*, 2551–2591.
Makowski, L. (1984) in *Biological Macromolecules and Assemblies* (Jurnak, F. A., & McPherson, A. M., Eds.) pp 203–253, Wiley-Interscience, New York.
Marvin, D. A., Bryan, R. K., & Nave, C. (1987) *J. Mol. Biol. 193*, 315–343.
Marzec, C. J., & Day, L. A. (1983) *Biophys. J. 42*, 171–180.
Marzilli, L. G., de Castro, B., Caradonna, J. P., Stewart, R. C., & Van Vuuren, C. P. (1980) *J. Am. Chem. Soc. 102*, 916–924.
Prescott, B., Steinmetz, W., & Thomas, G. J., Jr. (1984) *Biopolymers 23*, 235–256.
Putterman, D. G., Casadevall, A., Boyle, P. D., Yang, H.-L., Frangione, B., & Day, L. A. (1984) *Proc. Natl. Acad. Sci. U.S.A. 81*, 699–703.
Reisberg, S. A. (1988) Ph.D. Thesis, New York University, New York.
Simpson, R. B. (1964) *J. Am. Chem. Soc. 86*, 2059–2065.
Thomas, G. J., Jr. (1986) in *Spectroscopy of Biological Systems* (Clark, R. J. H., & Hester, R. E., Eds.) Adv. Spectrosc. Vol. 13, pp 233–309, Wiley, New York.
Thomas, G. J., Jr. (1987) in *Biological Applications of Raman Specroscopy* (Spiro, T. G., Ed.) Vol. 1, pp 135–201, Wiley, New York.
Thomas, G. J., Jr., & Barylski, J. R. (1970) *Appl. Spectrosc. 24*, 463–464.
Thomas, G. J., Jr., & Murphy, P. (1975) *Science (Washington, D.C.) 188*, 1205–1207.
Thomas, G. J., Jr., & Day, L. A. (1981) *Proc. Natl. Acad. Sci. U.S.A. 78*, 2962–2966.
Thomas, G. J., Jr., Prescott, B., & Day, L. A. (1983) *J. Mol. Biol. 165*, 321–356.
Thomas, G. J., Jr., Prescott, B., Opella, S. J., & Day, L. A. (1988) *Biochemistry* (submitted for publication).
Webster, R. E., Grant, R. A., & Hamilton, L. A. W. (1981) *J. Mol. Biol. 152*, 357–374.
Yamane, T., & Davidson, N. (1961) *J. Am. Chem. Soc. 83*, 2599–2607.
Young, P. R., Nandi, U. S., & Kallenbach, N. R. (1982) *Biochemistry 21*, 62–66.

Interactions of Oleic Acid with Liver Fatty Acid Binding Protein: A Carbon-13 NMR Study†

David P. Cistola,* Mary T. Walsh, Ronald P. Corey, James A. Hamilton, and Peter Brecher
Biophysics Institute, Housman Medical Research Center, Departments of Biochemistry and Medicine, Boston University School of Medicine, 80 East Concord Street, Boston, Massachusetts 02118
Received April 1, 1987; Revised Manuscript Received July 23, 1987

ABSTRACT: ^{13}C NMR spectroscopy was used to probe the structural interactions between carboxyl-^{13}C-enriched oleic acid (18:1) and rat liver fatty acid binding protein (FABP) and the partitioning of 18:1 between FABP and unilamellar phosphatidylcholine (PC) vesicles. Spectra of systems containing 2–8 mol of 18:1/mol of FABP (but no PC) exhibited one carboxyl resonance (182.2 ppm) corresponding to FABP-bound 18:1. At pH values <8.0, an additional carboxyl resonance, corresponding to unbound 18:1 in a lamellar phase, was observed. Both resonances exhibited ionization shifts with estimated apparent pK_a values of <5 (bound 18:1) and >7 (unbound 18:1). The intensity of the resonance corresponding to FABP-bound 18:1 increased with increasing 18:1/FABP mole ratio and at 8/1 mole ratio indicated that at least 2 and 6 mol of 18:1/mol of FABP were FABP-bound at pH 7.4 and 8.6, respectively. NMR spectra of systems containing equal concentrations (w/v) of FABP and PC and from 1 to 4 mol of total fatty acid (FA)/mol of FABP exhibited two 18:1 carboxyl resonances (182.2 and 178.5 ppm, pH 7.4). The downfield resonance corresponded to FABP-bound 18:1 and the upfield resonance to PC vesicle bound 18:1. At 1/1 mole ratio (FA/FABP), the intensities of both resonances were approximately equal, but at 4/1 mole ratio the resonance for PC vesicle bound 18:1 was 3-fold more intense than that for FABP-bound 18:1. The following conclusions are reached: (i) The carboxyl groups of 18:1 bound to liver FABP experience only one type of binding environment (the aqueous milieu adjacent to the protein surface). (ii) 18:1 bound to FABP is fully ionized at neutral pH, and the anionic 18:1 carboxyl groups are not involved in electrostatic interactions with cationic residues on FABP. (iii) Each mole of FABP bound at least 2 mol of 18:1 at physiological pH. However, in the presence of phospholipid vesicles, FABP bound up to 1 mol of 18:1/mol of FABP.

Fatty acid binding proteins (FABP)[1] are a class of abundant, low molecular weight cytosolic proteins that presumably function in the solubilization and transport of nonesterified fatty acids and their CoA derivatives within cells (Ockner et al., 1972). To aid in defining the functional role of FABP in vivo, the ligand binding properties of FABP have been exam-

† This work was supported by U.S. Public Health Service Grants HL-26335, HL-07291, and HL-31195. Preliminary accounts were presented at the 31st Annual Meeting of the Biophysical Society, New Orleans, LA, February 1987, and have been published in abstract form (Cistola et al., 1987c,d).

[1] Abbreviations: FABP, fatty acid binding protein(s); FA, fatty acid(s); 18:1, oleic acid and/or potassium oleate; TLC, thin-layer chromatography; PC, egg yolk phosphatidylcholine; P1, FABP preparation 1; P2, FABP preparation 2; T_1, spin–lattice relaxation time; NOE, nuclear Overhauser enhancement; CD, circular dichroic; UV, ultraviolet; Tris-HCl, tris(hydroxymethyl)aminomethane hydrochloride.

0006-2960/88/0427-0711$01.50/0